Carbohydrate Polymers 110 (2014) 505–512

Contents lists available at ScienceDirect

Carbohydrate Polymers

journal homepage: www.elsevier.com/locate/carbpol

Synthesis of a novel acrylated abietic acid-*g*-bacterial cellulose hydrogel by gamma irradiation

Muhammad Mustafa Abeer[a], Mohd Cairul Iqbal Mohd Amin[a,*], Azwan Mat Lazim[b], Manisha Pandey[a], Claire Martin[c]

[a] Centre for Drug Delivery Research, Faculty of Pharmacy, Universiti Kebangsaan Malaysia, Jalan Raja Muda Abdul Aziz 50300, Kuala Lumpur, Malaysia
[b] School of Chemical Sciences and Food Technology, Faculty of Science and Technology, Universiti Kebangsaan Malaysia, Bangi 43600, Selangor, Malaysia
[c] Department of Pharmacy, University of Wolverhampton, Wulfruna Street, Wolverhampton WV1 1LY, UK

ARTICLE INFO

Article history:
Received 3 December 2013
Received in revised form 14 April 2014
Accepted 17 April 2014
Available online 25 April 2014

Keywords:
Bacterial cellulose
Abietic acid
Hydrogel
Gamma radiation
Polymer

ABSTRACT

Acrylated abietic acid (acrylated AbA) and acrylated abietic acid-grafted bacterial cellulose pH sensitive hydrogel (acrylated AbA-*g*-BC) were prepared by a one-pot synthesis. The successful dimerization of acrylic acid (AA) and abietic acid (AbA) and grafting of the dimer onto bacterial cellulose (BC) was confirmed by ^{13}C solid state NMR as well as FT-IR. X-ray diffraction analysis showed characteristic peaks for AbA and BC; further, there was no effect of increasing amorphous AA content on the overall crystallinity of the hydrogel. Differential scanning calorimetry revealed a glass transition temperature of 80 °C. Gel fraction and swelling studies gave insight into the features of the hydrogel, suggesting that it was suitable for future applications such as drug delivery. Scanning electron microscopy observations showed an interesting interpenetrating network within the walls of hydrogel samples with the lowest levels of AA and gamma radiation doses. Cell viability test revealed that the synthesized hydrogel is safe for future use in biomedical applications.

1. Introduction

Cellulose-based hydrogels have been synthesized and studied for diverse applications. Water-soluble derivatives of cellulose have frequently been used to form hydrogels, by using only the cellulose derivative or by using its polymer blend with other natural or synthetic polymers (Chang & Zhang, 2011; Edgar, 2007). Hydrogels of water-soluble cellulose derivatives such as carboxymethyl cellulose and hydroxypropylmethyl cellulose are synthesized by exposing a paste (10%, w/v or above) of the cellulose derivatives to high-energy ionizing radiation (Pekel, Yoshii, Kume, & Güven, 2004; Yoshii et al., 2003). These hydrogels, among others, have been used in a variety of biomedical applications such as tissue engineering scaffolds and drug delivery systems, and are obtained from guar gum, pectin, chitosan, and dextran (Shukla & Tiwari, 2012). Hydrogels based on native cellulose can be prepared by dissolving cellulose in a solvent with or without water-soluble vinyl monomers such as acrylic acid (AA) and acrylamide. Hydrogels composed solely of hydrophilic vinyl monomers are considered as first-generation/conventional super-porous hydrogels. However, because of their poor mechanical properties, these hydrogels do not form products that are mechanically sustainable under stress, and are not suited for skin or oral applications (Mastropeitro, Omidian, & Park, 2012). In order to overcome this issue, these hydrogels have been combined with native bacterial cellulose (BC) for obtaining superior mechanical, swelling, and stimuli-responsive properties. Recently, syntheses using micronized BC with electron beam irradiation and BC flakes with microwave irradiation have followed the aforementioned theme (Amin, Ahmad, Halib, & Ahmad, 2012; Halib, Amin, & Ahmad, 2009; Pandey & Amin, 2013). Cellulose has also been combined with organic compounds, and this is in contrast to its combination to synthesize hydrogels with water-soluble vinyl monomers mentioned earlier. An exemplary study reported the combination of the ester of dehydroabietic acid with cellulose. In the study, the O-acylation reaction was conducted in an ionic liquid to yield cellulose dehydroabietate, which had better solubility and better resistance to acids and bases as compared to native cellulose (Xu, Duan, Huang, & Li, 2011). Abietic acid (AbA) is another organic resin acid that has been combined with hydroxypropylcellulose to form a macromolecular pro-drug through formation of ester linkage (Hussain, 2007). AbA constitutes more than 90% of the rosin along with dehydroabietic acid and isomeric L-pimaric acid (Wang, Yao, Wang, Tang, & Jiang, 2013). It is a monocarboxylic acid

* Corresponding author.
E-mail address: mciamin@pharmacy.ukm.my (M.C.I.M. Amin).

http://dx.doi.org/10.1016/j.carbpol.2014.04.052
0144-8617/

substituted phenantherene (a bulky hydrophobic moiety), which has various applications including synthesis of various bioactive molecules, preparation of pellets of drugs with retarded release and block copolymers for the synthesis of micellar nanoparticles for drug delivery (Abdulla, 2008; Nande, Barbade, Morkhade, Patil, & Joshi, 2006; Wang et al., 2013).

L-Pimaric acid (LPA), an isomer of AbA that differs only in the site of saturation within the phenantherene nucleus, has been dimerized with AA to form acrylated L-pimaric acid (Bicu & Mustaţa, 2007). This bi-functional compound furthered the esterification of isomeric levopimaric acid, a reaction otherwise reported as difficult to carry out. The esterification of acrylated LPA was carried out with ethylene carbonate (1,3-dioxolan-2-one) (Mustata & Bicu, 2010). These studies show that chemical modification of AbA and its isomers precedes polymer synthesis in the generation of novel materials with different applications. Modified AbA can also be used to synthesize hydrogels (swollen cross-links) i.e. in contrast to the aforementioned non-swelling polymers. Chiral hydrogels have been obtained using AbA derivatives. They retain the configuration of the parent L-abietic acid, whereby AbA acts as the source of chirality for *N*-propargyl abietamide, the copolymer, and its hydrogel with achiral moieties such as *N*-isopropyl acrylamide (NIPAam). The hydrogel showed considerable enantioselective recognition toward molecules with the L-configuration (Yao, Zhang, Zhang, Yang, & Dang, 2013). Such hydrogels have been reported and prepared by combining native BC with AA. The combination of LPA and AA has also been reported in the synthesis of the subsequent polymer. However, the synthesis of hydrogels with AbA or modified AbA, AA, and cellulose has not been reported.

In this study, we aimed to synthesize and characterize acrylated AbA and graft it onto BC to form a hydrogel. We then evaluated the cytocompatibility of the hydrogel. The proposed synthesis of the hydrogel is a one-pot process, as the modification of AbA and the grafting of acrylated AbA onto BC can be effected in the same reaction.

2. Experimental

2.1. Materials

Nata de coco was obtained from the local food market. AbA (85%) was obtained from Acros Chemicals, Belgium. AA was procured from Sigma Aldrich (St. Louis, MO, USA). All reagents were of analytical grade and used without further purification (except *nata de coco*).

2.2. Preparation of microfibrillated BC (MFBC)

BC was prepared according to a previously reported method (Amin, Abadi, Ahmad, Katas, & Jamal, 2012). Briefly, food-grade *nata de coco* was subjected to acid removal by soaking in water until a neutral pH was obtained. Next, it was treated with 0.1 N NaOH solution in a hot water bath for 1 h at 90 °C. After the pH became neutral, the mixture was lyophilized and finally ground to microfibrillated BC using a *Pulverisette 14* (Fritsch, Idar-Oberstein, Germany) rotor mill.

2.3. Synthesis of acrylated AbA and acrylated AbA-g-bacterial cellulose hydrogel

An aqueous dispersion (1%, w/v) of the microfibrillated BC (300–600 μm) was obtained by mechanical homogenization at 11,000 rpm with a mechanical homogenizer (IKA Labortechink Ultra Turrax T25, Germany). To produce three different aqueous dispersions, 3 g of AbA (0.01 mol) and three different volumes of AA (20.58 ml (0.3 mol), 27.45 ml (0.4 mol), and 34.03 ml (0.5 mol)) were added separately to make up the volume of the BC aqueous dispersions to 100 mL. Homogenization was continued until no phase separation was observed. The three formulations were irradiated in an oxygen-rich atmosphere at radiation doses of 30 kGy, 40 kGy, and 50 kGy with a *Gammacell 220* ^{60}Co radiation source (Maximum activity; 410Tbq, Dose rate; 2.076 kGy/h). Hydrogels were named according to the different volumes of AA and radiation doses used (Table 1).

2.4. ^{13}C solid state NMR

The selected hydrogel sample was purified in distilled water. It was freeze-dried and finely ground to make it suitable for ^{13}C NMR analysis in solid state. Solid-state cross-polarization/magic angle spinning (CPMAS) ^{13}C NMR spectra of the hydrogel was recorded using an NMR spectrometer (Avance 400; Bruker, Germany). A 100 mg of the sample was packed into the 4-mm inner diameter cylindrical zirconium oxide MAS rotor with an O-ring seal and end cap. Chemical shifts were recorded in ppm with reference of 29.50 ± 0.10 ppm (CH) and 38.56 ± 0.10 ppm (CH_2) using adamantine as the external standard.

2.5. FT-IR analysis

All the freshly prepared hydrogels were placed in distilled water, such that the distilled water was replaced twice a day for two weeks to ensure removal of any possible un-reacted monomers present and only purified hydrogel would be available for analysis. Afterwards the hydrogels were freeze-dried and powdered. The FT-IR samples were prepared by mixing the powder in KBr and fusing the mixture into a transparent disc using a hydraulic press. The FT-IR analysis was performed by using an FT-IR spectra 2000 spectrophotometer (Perkin-Elmer, Waltham, USA) under the following conditions: range: 4000–500 cm^{-1}, resolution: 4 cm^{-1}, number of accumulation scans: 16.

2.6. Differential scanning calorimetry (DSC)

The hydrogel samples were studied using a Diamond differential scanning calorimeter (Perkin-Elmer, Waltham, USA). For analysis, 5 mg of each sample was sealed in an aluminum pan specifically meant for solid samples. The samples were analyzed over the temperature range 0–200 °C at a rate of 20 °C/min and a nitrogen purge of 25 mL/min.

2.7. Scanning electron microscopy (SEM)

The hydrogels were cut into circular discs and freeze-dried prior to the porosity analysis. The samples were coated by using a gold sputter coater under an argon atmosphere and mounted onto the aluminum stub of a LEO 1450 VP scanning electron microscope. Images were recorded at different magnifications.

2.8. Gel fraction

The freshly prepared hydrogels were cut into discs, which were then dried in an oven at 60 °C until they reached a constant weight. The samples were purified by soaking in distilled water for a week. The soaking water was replaced with fresh distilled water at every 12 h in order to remove any un-reacted monomers. Subsequently, the hydrogels were removed and dried overnight after a week. Then, the final weight was measured and the gel fraction was obtained using the following equation:

$$\frac{W_f}{W_i} \times 100$$

Table 1
Sets and gel fraction of hydrogel formulations based on different volumes of acrylic acid and radiation doses used.

Formulation code	Radiation dose (kGy)	Components of hydrogel formulation			Gel fraction (g/g %) mean ± S.D. (n = 3)
		Acrylic acid (ml)	Abietic acid (g)	Bacterial cellulose dispersion[a] (%, w/v)	
H130	30	20.5	3	1	73 ± 1.0
H140	40				75 ± 1.8
H150	50				83 ± 1.9
H230	30	27.4			72 ± 0.9
H240	40				76 ± 1.5
H250	50				78 ± 1.0
H330	30	34.3			72 ± 0.6
H340	40				78 ± 1.3
H350	50				81 ± 1.8

[a] Volume of dispersion containing all the three ingredients together was made up to 100 ml with distilled water (q.s.).

where W_i and W_f denote the weight before and after extraction, respectively.

2.9. Swelling studies

Swelling studies were conducted with phosphate buffer saline (PBS) solutions of pH 2.0, 5.0, 7.0, and 10.0 at room temperature. The pH was adjusted with 1.0 M HCl or 1.0 M NaOH. The dried samples were weighed and soaked in the respective solutions, and then, the weights were noted at certain time intervals. All the measurements were performed in triplicate. Before weighing, the excess solution on the surface of the soaked sample was blotted off with filter paper. The swelling ratio was determined as follows:

$$\frac{W_s - W_d}{W_d} \times 100$$

where W_s is the weight of the swollen hydrogel and W_d is the weight of the dried hydrogel.

2.10. X-ray diffraction (XRD) analysis

X-ray diffraction analysis was performed using a D8-Advance diffractometer (Bruker AXS, Mannheim, Germany). BC, AA, AbA, and hydrogel samples were ground as finely as possible and loaded onto the nine-chambered port of the diffractometer. The analysis was conducted over the 2θ range 0–70° using CuKα radiation, at 40 kV and 50 mA.

2.11. Cell viability

The V79 (Chinese hamster lung fibroblast) cell line was obtained from ATCC (Manassas, VA, USA) and used to assess the cell viability of the hydrogel samples. V79 cells were cultured in Dulbecco's modified eagle medium (DMEM) (*Gibco*™ by *Life* Technologies, USA) supplemented with 10% fetal bovine serum (FBS) (Sigma Aldrich, USA) and 1% penicillin-streptomycin (Thermo-Fisher Scientific, USA). The cells were maintained at 37 °C in a humidified atmosphere with 5% CO_2. The cells were seeded at a density of 30,000 cells/well in a 96-well plate. Hydrogel sample extracts were prepared by rinsing the hydrogel with PBS. In addition to the cells, these extracts were also incubated prior to cell seeding (Ku, Sfier, & Kumta, 2010; Kumar et al., 2011). The initial concentration of the inoculated samples was 2 mg/mL, which was serially diluted five times to obtain a range of concentrations at which the effects of every set of hydrogels on cell viability could be observed. After incubating with hydrogels and achieving the desired growth, cells were incubated with 20 μL of Alamar blue® (Invitrogen, Carlsbad, CA, USA) for 4 h (Amjad, Amin, Katas, & Butt, 2012). The absorbance at 570 nm was noted after 24 h and 48 h using an Infinite® M200 pro Nanoquant (Tecan, Switzerland) microplate reader. The percent cell viability was calculated using the following formula:

$$\%\,\text{cell viability} = \left(\frac{A_{570}\text{ of cells with hydrogel}}{A_{570}\text{ control}}\right) \times 100$$

2.12. Statistical approaches

SPSS 15.0 for windows (evaluation version, IBM Corporation, Armonk, New York, USA) was used to analyze the data. The data are presented as the average ± standard deviation (SD). One-way *ANOVA* was employed to observe significant differences wherever applicable. $p < 0.05$ was taken as the significant value. The post hoc Tukey test was employed for cell viability analysis.

3. Results and discussion

3.1. Synthesis of acrylated AbA and acrylated AbA-g-bacterial cellulose hydrogel

Aqueous dispersions containing AA, AbA, and BC were subjected to gamma radiation and left overnight until the samples reached the final cross-linked forms. The obtained hydrogel is shown in Fig. 1. The hydrogel had a yellowish hue because of the presence of AbA, which is yellow in color.

3.2. CP/MAS ^{13}C NMR

Solid state CP/MAS ^{13}C NMR analysis was conducted as the hydrogel samples are insoluble in the common solvents used for NMR analysis. Fig. 2(A) shows 400 MHz ^{13}C NMR spectrum of the

Fig. 1. Acrylated AbA-*g*-BC hydrogel synthesized at 30 kGy (H130, 0.3 mol of AA).

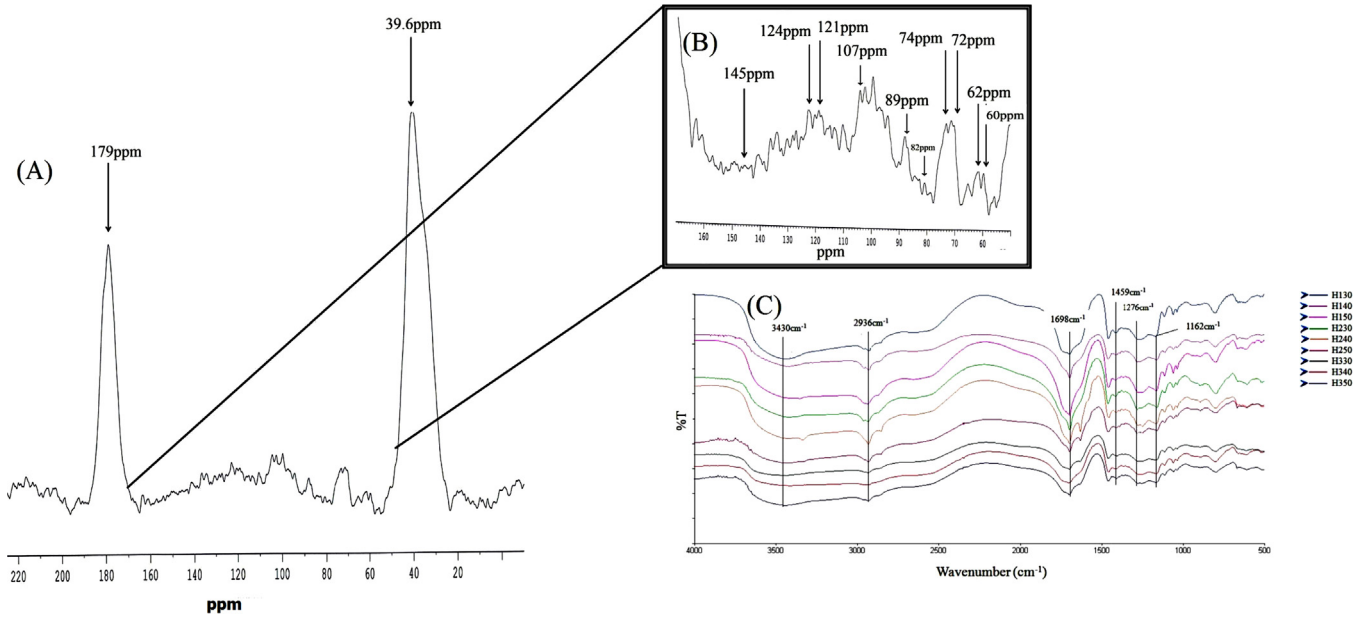

Fig. 2. (A) ^{13}C NMR analysis of H130 sample of acrylated AbA-*g*-BC hydrogel. Two major peaks at 179 ppm and 39.6 ppm can be seen for —COO and —CH_2 found in the hydrogel. (B) Magnified image on the scale between 170 ppm and 50 ppm represents characteristic peaks for dimerized AbA (145, 124, 121, and 55 ppm) and grafting on BC backbone (62, 60 ppm) (C) FT-IR spectra representing the essential peaks of dimerization between AA and AbA and grafting of the adduct onto BC.

freeze-dried acrylated AbA-*g*-BC hydrogel (H130). The data generated confirmed the formation of acrylated AbA and its grafting on BC backbone as shown in Fig. 2(B). A characteristic peak on 62 ppm confirms grafting of the acrylated AbA on BC backbone. The peak at 62 ppm refers to C6 of anhydroglucose unit in cellulose. The hydroxyl group attached to this carbon actually contributes toward graft reaction. The peak at 62 ppm represents substituted hydroxyl groups. However, the peak at 60 ppm is sometimes found and represented as a doublet peak with 62–63 ppm. It is consistent with a finding that the peak at 60 ppm appears as doublet chemical shift after grafting reaction has taken place (Guo, Liu, et al., 2013; Guo, Wang, Shen, Shu, & Sun, 2013). Typical peaks for cellulose backbone are also found in the NMR spectrum, i.e. 72 ppm and 74 ppm corresponding to C2, C3 and C5. Peaks at 82 ppm and 89 ppm represent the amorphous and crystalline C4 carbons of BC backbone (Foston, 2014). Peak at 107 ppm represents C1 of BC backbone. The formation of acrylated AbA is confirmed by various peaks corresponding to the carbons of the dimers. Peaks appeared at 145, 124, 121 and 55 ppm correspond to C2, C3, C4 and C5 of the dimerized AbA respectively. The data obtained is similar to the one generated for acrylated LPA, where LPA differs only in the site of saturation from AbA within phenanthrene nucleus (Bicu & Mustaţa, 2007). All —CH_2 groups of acrylated abietic acid are shown by one broad peak shown at 39.6 ppm. The carboxyl groups of the dimer having abietic acid and acrylic acid are shown at 179 ppm (Liu, Xin, & Zhang, 2009; Spoljaric, Salminen, Luong, & Seppälä, 2013).

3.3. FT-IR analysis

The FT-IR spectra as in Fig. 2(C) confirms the dimerization between AA and AbA, followed by the side chain propagation of AA and grafting onto BC. Some typical peaks were obtained at 3400 [υ (OH) in COOH], 2936 [υ (C—H) in pyranoid ring), 1698 [υ (C=O) in COOH of both of AA and AbA], 1459 [δ (CH_3) in isopropyl group], 1276 [δ (OH) dimer], 1162 [υ (C—O—C ether linkage in BC backbone)]. These data correlate well with the data obtained via the chemical method for the acrylated L-pimaric acid adduct (Bicu & Mustaţa, 2007). Since L-pimaric acid is an isomer of AbA and differs only in the site of saturation within the phenanthrene nucleus, the aforementioned results confirmed that acrylation of AbA had occurred; the peaks for the dimer, isopropyl group, and hydroxyl group were the same as those for the acrylated LPA. Moreover, the presence of the ether linkage confirmed the presence of chemically linked BC in the formulation. This is in accordance with the fact that BC can be modified chemically to achieve different morphologies and properties. The absence of C—O stretching vibrations confirmed that the dimer was grafted through AA on the backbone (Xu, Duan, Huang, & Li, 2011).

3.4. Reaction mechanism

FT-IR and NMR data revealed all the peaks that serve as evidence for the formation of the adduct between AbA and AA. After the generation and attack of free radicals, acrylated AbA was formed. Once dimerized, it acted as the site for extension of the AA side chain. Cross-linking of the AA side chain of AbA to form the polyacrylic acid (PAA) side chain was also mediated by free radicals. The polymerized AA cross-linked side chain worked as a bridge between AbA and the BC backbone and as a graft for the reaction site generated by free radicals on the BC polymer (Fig. 3).

3.5. Scanning electron microscopy

SEM images were recorded at various magnifications to estimate the range of pore sizes for the different sets of hydrogels. Notably, the sample at 30 kGy showed characteristic interpenetrating pores on the order of 5–7 μm within the walls of the larger pores. Such a pattern was not observed in any of the samples with higher doses of radiation at the same concentration of AA or with higher doses of radiation and higher concentrations of AA. The larger pores were about 300–400 μm in diameter (Fig. 4). The pore density appeared to decrease with an increase in radiation dose. SEM micrographs revealed a decrease in the pore network at increased radiation doses. Fewer pores and smaller pore sizes were attributed to the increased probability of cross-linking at higher radiation doses and higher AA concentrations. The overall morphology of the formed hydrogel was sponge-like, which allowed for diffusion and remained unaffected by the radiation

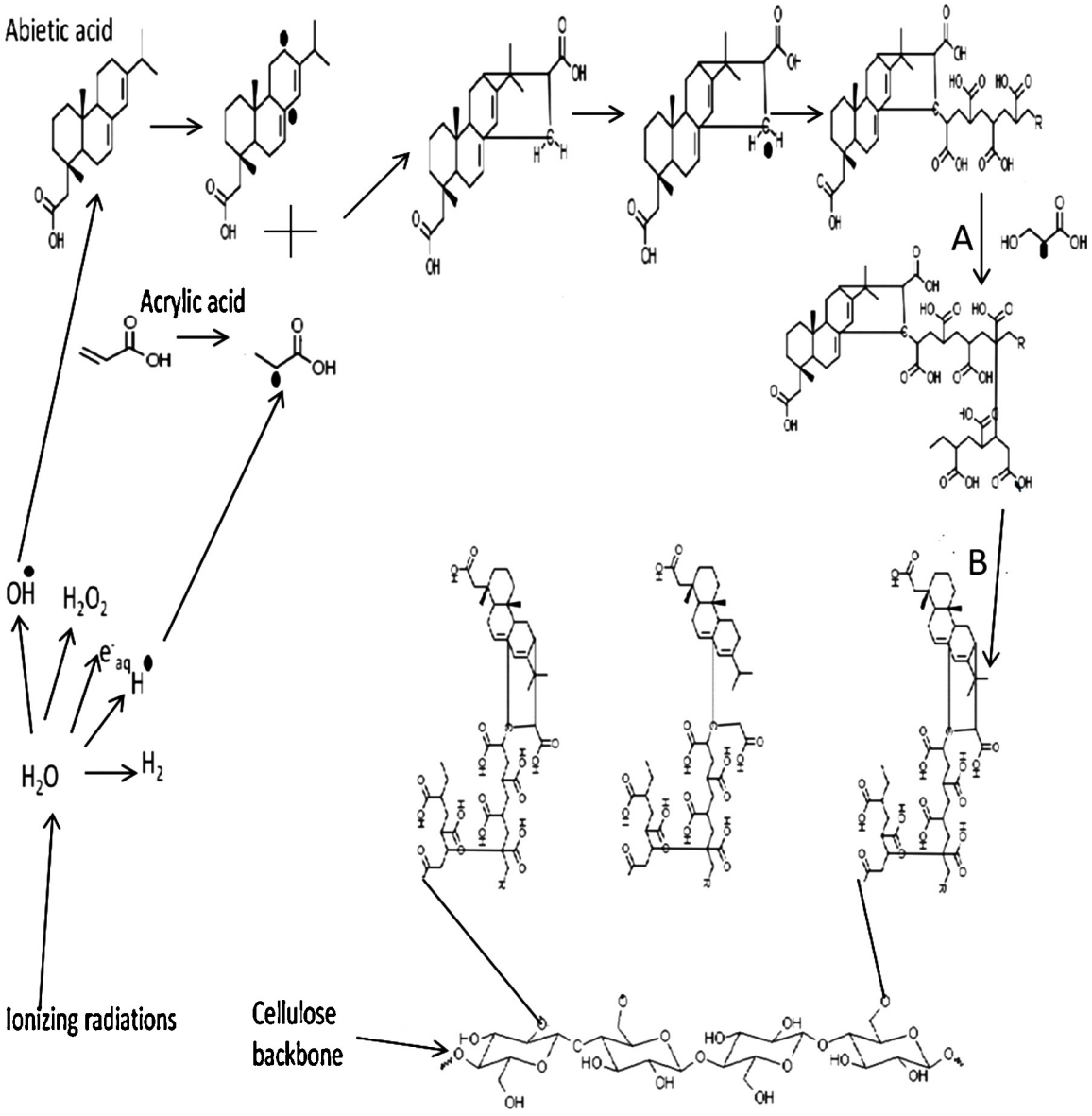

Fig. 3. Free radical-mediated synthesis of acrylated AbA & acrylated AbA-*g*-BC hydrogel. A represents cross-linking of the polyacrylic acid side chain (PAA) attached to the dimer, mediated by acylic acid radical form. B represents the grafting of the dimer through cross-linked PAA side chain on the radical generated reactive site on cellulose backbone.

level. The minimum pore size obtained in the study was similar to the pore size of hydrogels used in drug delivery (Amin, Ahmad, Halib, & Ahmad, 2012). The observed morphology also supported the notion of the hydrogels as super porous hydrogels (SPH) as they resembled third-generation SPHs. These hydrogels have extraordinary pore networks, show exponential swelling, and do not use swellable fillers (Mastropeitro, Omidian, & Park, 2012; Zhang et al., 2011).

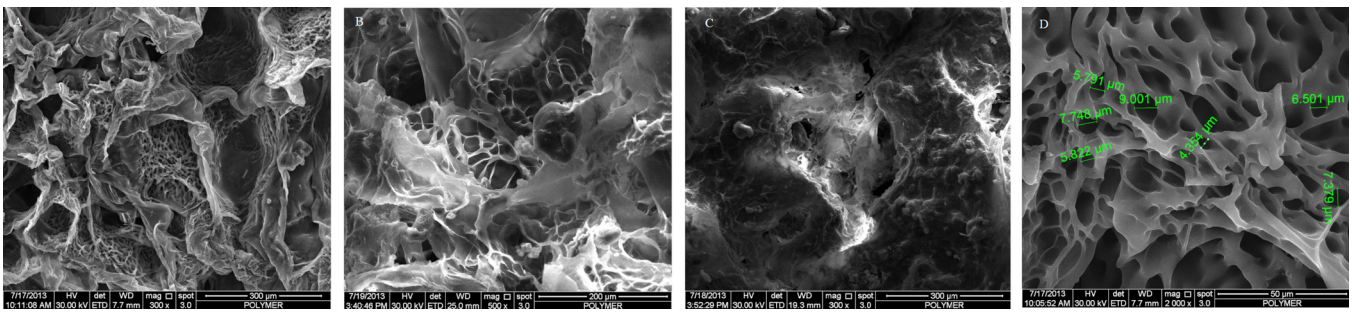

Fig. 4. A to C show a decrease in porosity with an increase in radiation dose where A also shows the interpenetrating pores within the walls of the larger pores in the samples irradiated at 30 kGy. D shows the size of the pores within the walls of larger pores.

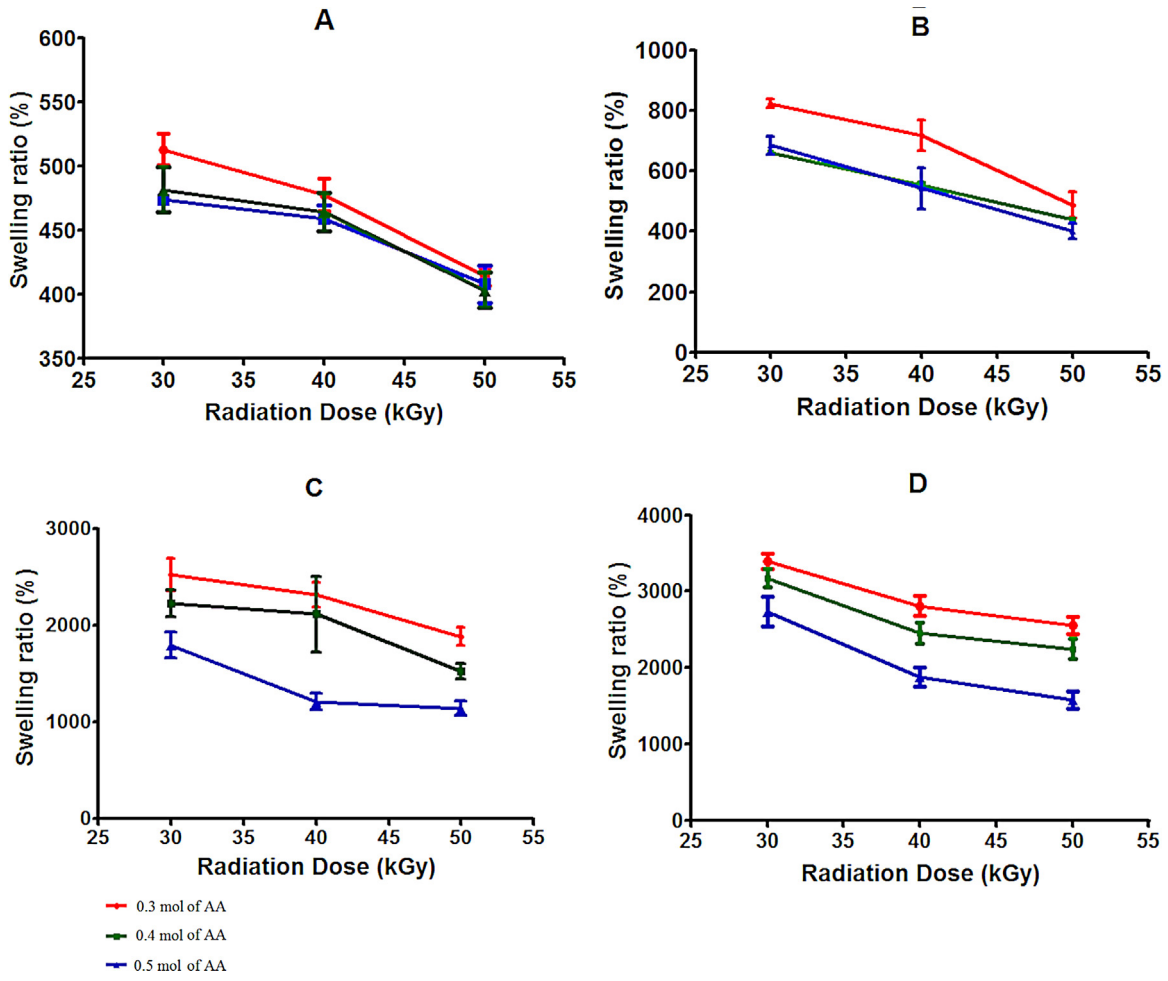

Fig. 5. Swelling ratios at pH: A (2.0), B (5.0), C (7.0), D (10.0). Swelling increased with increasing pH regardless of the acidic or basic pH. Swelling decreased with the increase in radiation dose to which formulations were exposed for synthesis of hydrogels with different concentrations of AA. Data are expressed as mean ± S.D., $n = 3$.

3.6. Gel fraction

Gel fraction percentages were calculated from the given formula. Gel fractions were in the range 73.0 ± 1.0 to 83.0 ± 1.9. The compact range of values could be attributed to the presence of AbA, because previously reported hydrogels based on BC and AA had a broader gel fraction range and the maximum gel fraction was higher than that obtained here, as shown in Table 1. There was an increase in the gel fraction (%) with increasing radiation dose. However, no significant difference was observed between samples with different AA concentrations, as indicated by $p = 0.8665$. Therefore, increasing concentrations of AA did not increase the gel fraction.

3.7. Swelling studies

The acrylated AbA-*g*-BC hydrogel was found to be pH responsive. The swelling ratio (%) was the lowest at pH 2.0 (average swelling ratio of 400%) and increased monotonically with pH (from acidic to basic), unlike hydrogels without AbA, which showed reduced swelling at pH > 7.0. This modification is encouraging for potential applications involving greater but controlled drug release at intestinal pH. The swelling ratio (%) was found to decrease with an increase in the radiation dose (Halib, Amin, & Ahmad, 2010). The maximum swelling ratio (%) was about 3200% after reaching equilibrium within 24 h at pH 10.0 for H130 (Fig. 5). The reduced swelling at pH 2.0 was due to the lack of deprotonation of the carboxyl groups of AA. However, the number of available free carboxyl groups for swelling seemed to be independent of the AA concentration, as there was no significant variation between the swelling ratio percent of hydrogels with higher AA concentrations. The swelling ratio at all pH values differed significantly as a function of radiation dosage. The p values for the data set of the pH values at different radiation doses suggested by one way ANOVA were less than 0.05. Hydrogels with AbA were distinguished from similar hydrogels on the basis of the decreased overall swelling. Specifically, in earlier studies with BC and AA, the swelling ratio increased up to 6000% (Amin, Ahmad, Halib, & Ahmad, 2012). AbA has been used to increase the water resistance of materials in a number of studies. Actually, AbA led to the introduction of hydrophobic domains and probably suppressed the diffusion of water during the early stages of swelling. It is established that if resins such as AbA are introduced into the formulation, the amount of water entering the hydrogel is decreased (Lee & Yeh, 2005; Nande, Barabde, Morkhade, Patil, & Joshi, 2006).

3.8. X-ray diffraction analysis

All the hydrogel samples were analyzed to elucidate their crystallinity. The hydrogels had two distinct peaks at $2\theta = 10^\circ$ and 16° and a less sharp, yet observable peak at about 22.5° (Fig. 6B–D). AbA itself has an extraordinary crystalline structure, and most of the peaks in the XRD spectrum were in the range $2\theta = 10$–20°. All the peaks in this range were diminished in the XRD spectrum of the hydrogel, except for the significant peak at 10°. This peak can

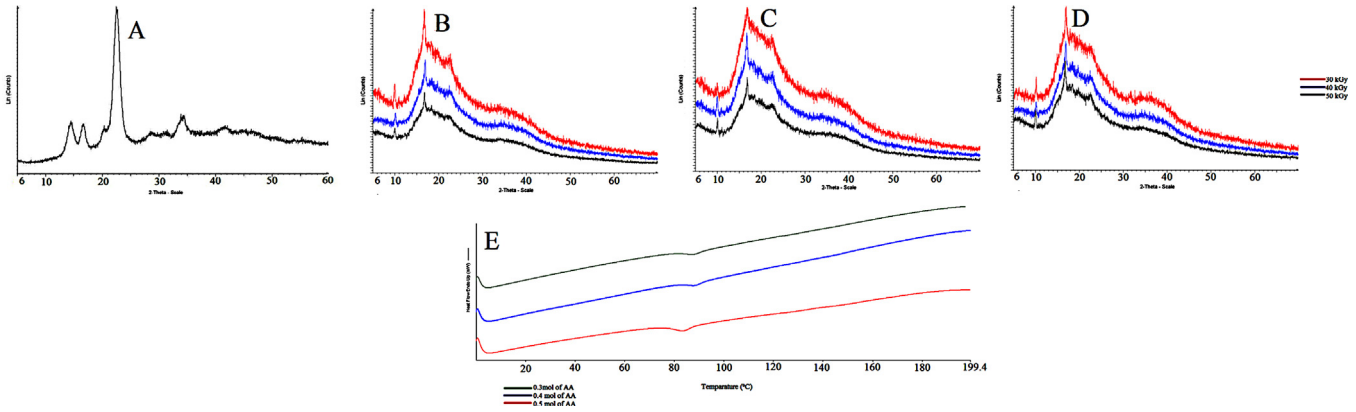

Fig. 6. A shows the XRD pattern for pure BC. B, C and D show XRD patterns for the samples with 0.3, 0.4 and 0.5 mol of AA respectively. No effect of changing AA concentration was observed on overall crystallinity of the hydrogel. E represents DSC thermograms of hydrogels with 0.5 mol of AA, where glass transition temperature can be seen a little above 80 °C.

be seen in a comparison of the reported peaks of the coarse resin (a mixture of all resin acids) which was at 12° for the microparticles (Lee et al., 2004). The decrease in crystallinity confirmed that AbA had been incorporated into the hydrogel structure (Lee et al., 2005). The peak at $2\theta = 16.5°$ corresponded to the (1 0 1) crystallographic plane of the diffractogram for BC. The broad peak observed at 22.5° corresponded to the (0 0 2) plane. However, the characteristic peaks of BC were not seen in the final hydrogel, indicating the grafting and disruption of the secondary structure of BC. The peak seems to be in agreement with the studies reported earlier and confirms the presence of BC as a backbone for grafting. An increase in AA concentration did not affect the overall crystallinity, which confirmed that increasing amorphous zones do not alter the crystallinity of cellulose or its hydrogels (Zhao et al., 2007).

3.9. Differential scanning calorimetry

DSC was performed to estimate the glass transition temperature (T_g). T_g was only observable for the endothermic peaks of samples with the highest AA concentration and was about 80 °C for the three samples as shown in Fig. 6(E). This was in agreement with the softening point reported for rosin microparticles, which increased from 70.5 °C to 80.6 °C on the addition of the hydrophobic moiety, indomethacin (Lee et al., 2004). The T_g value was higher than that reported for previously synthesized AA-*g*-BC hydrogels, probably because the acrylated AbA-*g*-BC hydrogel has a molecular weight larger than that of the previously reported AA-*g*-BC hydrogel because of the presence of AbA. As the molecule becomes larger, it requires more energy and higher temperatures to vibrate. Furthermore, water resistance played a role in increasing T_g as compared to that of AA-*g*-BC hydrogels. Water acts as a plasticizer and when the bound fraction of water increases, T_g decreases. Hence, AbA imparted water repellence to the hydrogels investigated in the present study, as shown by the higher T_g. A high concentration could also be a possible explanation, as T_g is affected by the degree of polymerization, which is in turn affected by the amount of monomer used.

3.10. Cell viability test

This study was conducted in order to investigate cytocompatibility of the material as a new combination could be cytotoxic,

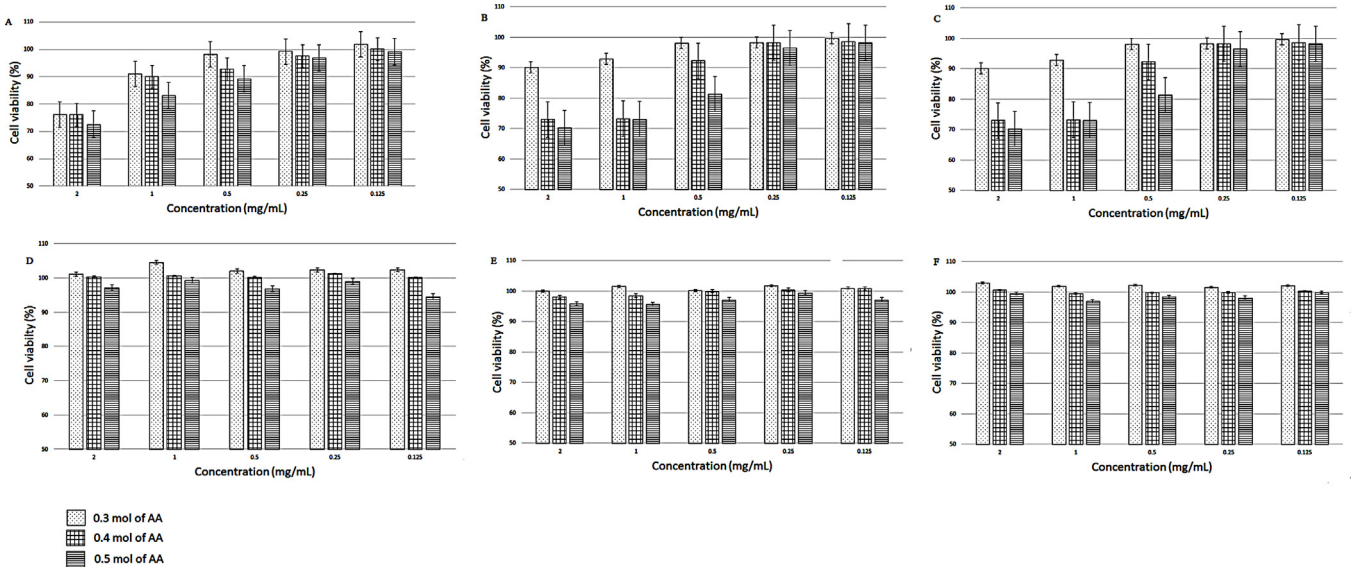

Fig. 7. A–C represent the samples with different acrylic acid concentration at 30 kGy, 40 kGy and 50 kGy respectively for 24 h. Within every group of hydrogel concentration (mg/mL) a decrease in cell viability is observed due to increase in AA concentration at a specific radiation dose. Data are expressed as mean ± S.D., $n = 3$ and analyzed with one-way Anova and Tukey test. D–F represent the samples with different acrylic acid concentration at 30 kGy, 40 kGy and 50 kGy respectively for 48 h. Increase in growth at highest hydrogel concentration, i.e. 2 mg/mL was observed in contrast to A–C which confirmed that hydrogel allowed the cells to grow on extended span of time. Data are expressed as mean ± S.D., $n = 3$ and analyzed with *One-way Anova* and Tukey test.

regardless of the inertness of the starting materials (Wang, Li, Xing, Dong, & Gao, 2012). To evaluate the safety associated with the use of this hydrogel in future applications, the easily reproducible V79 cell line was cultured. An indirect method was adopted for the viability tests, whereby the hydrogel sample extracts were incubated with the culture medium. This approach had to be used because powdered hydrogel particles swelled when exposed to the medium, following seeding of the cells, and aggregated instead of coming in contact with the target cells.alamar Blue® assay was conducted to view changes in the metabolic activities of the cells and to determine the overall percentage of viable cells. The reduction of resazurin to resorufin by viable cells was used to quantify the cell viability in the presence of test samples. The minimum cell viability (%) was found to be about 72% for the H130 sample at 2 mg/mL by performing absorbance measurements in 24 h intervals. Cell viability appeared to decrease with an increase in the AA content and was observed for test sample concentrations ranging from 2 mg/mL to 0.125 mg/mL. This may be because increased AA content results in an acidic environment and thus causes cell destruction (Gupta, Plummer, Bisson, Frey, & Hilborn, 2002). However, the decrease in cell viability was acceptable, as the minimum cell viability was very good even at 2 mg/mL for all the hydrogel samples. The concentration ranges tested in this study are way below the IC_{50} value. After 24 h, cell viability seemed to increase slightly in samples with higher radiation doses, but after 48 h, this effect was diminished (Fig. 7). This observation indicated that increased radiation had no marked effect on cell viability. Therefore, it was confirmed that the combination of BC and AbA was inert, similar to single-component systems.

4. Conclusion

We report for the first time the synthesis of acrylated AbA and its hydrogel with BC and determine the pH sensitivity of the hydrogel. The use of ionizing radiation appears to be an alternative to the previously reported methods for the synthesis of acrylated resins. We evaluated the novel hydrogel as a candidate for future drug delivery applications in terms of the appropriate porosity, gel fraction, swelling properties, and biocompatibility.

Acknowledgement

The authors would like to thank the Ministry of Education, Malaysia (FRGS/1/2013/SKK02/UKM/02/3) for their financial assistance and support.

References

Abdulla, M. M. (2008). Anti-inflammatory activity of heterocyclic systems using abietic acid as starting material. *Chemical Monthly*, *139*, 697–705.
Amin, M. C. I. M., Abadi, A. G., Ahmad, N., Katas, H., & Jamal, A. J. (2012). Bacterial cellulose film coating as drug delivery system: Physicochemical, thermal and drug release properties. *Sains Malaysiana*, *41*, 561–568.
Amin, M. C. I. M., Ahmad, N., Halib, N., & Ahmad, I. (2012). Synthesis and characterization of thermo- and pH-responsive bacterial cellulose/acrylic acid hydrogels for drug delivery. *Carbohydrate Polymers*, *88*, 465–473.
Amjad, M. W., Amin, M. C. I. M., Katas, H., & Butt, A. M. (2012). Doxorubicin-loaded cholic acid-polyethyleneimine micelles for targeted delivery of antitumor drugs: Synthesis, characterization, and evaluation of their in vitro cytotoxicity. *Nanoscale Research Letters*, *7*, 687–695.
Bicu, I., & Mustaţa, F. (2007). Polymers from a Levopimaric acid–acrylic acid diels–alder adduct: Synthesis and characterization. *Journal of Polymer Science: Part A: Polymer Chemistry*, *45*, 5979–5990.
Chang, C., & Zhang, L. (2011). Cellulose based hydrogels: Present status and application prospects. *Carbohydrate Polymers*, *84*, 40–53.
Edgar, K. J. (2007). Cellulose esters in drug delivery. *Cellulose*, *14*, 49–64.
Foston, M. (2014). Advances in solid state NMR of cellulose. *Current Opinion in Biotechnology*, *27*, 176–184.
Guo, Y., Liu, Q., Chen, H., Wang, X., Shen, Z., Shu, X., et al. (2013). Direct grafting modification of pulp in ionic liquids and self assembly of the graft copolymers. *Cellulose*, *20*, 873–884.
Guo, Y., Wang, X., Shen, Z., Shu, X., & Sun, R. (2013). Preparation of cellulose-graft-poly(ε-caprolactone) nanomicelles by homogeneous ROP in ionic liquid. *Carbohydrate Polymers*, *92*, 77–83.
Gupta, B., Plummer, C., Bisson, I., Frey, P., & Hillborn, J. (2002). Plasma-induced graft polymerization of acrylic acid onto poly(ethylene terephthalate) films: Characterization and human smooth muscle cell growth on grafted films. *Biomaterials*, *23*, 863–871.
Halib, N., Amin, M. C. I. M., & Ahmad, I. (2009). Swelling of bacterial cellulose-acrylic acid hydrogels: Sensitivity towards external stimuli. *Sains Malaysiana*, *38*, 785–791.
Halib, N., Amin, M. C. I. M., & Ahmad, I. (2010). Unique stimuli responsive characteristics of electron beam synthesized bacterial cellulose/acrylic acid composite. *Journal of Applied Polymer Science*, *116*, 2920–2929.
Hussain, M. A. (2007). Unconventional synthesis and characterization of novel abietic acid esters of hydroxypropylcellulose as potential macromolecular prodrugs. *Journal of Polymer Science: Part A Polymer Chemistry*, *46*, 747–752.
Ko, H., Sfeir, C., & Kumta, P. N. (2010). Novel synthesis strategies for natural polymer and composite biomaterials as potential scaffolds for tissue engineering. *Philosophical Transactions of the Royal Society A*, *368*, 1981–1997.
Lee, C., Lim, S., Kim, G., Kim, D., Kim, D. W., Lee, H., et al. (2004). Rosin microparticles as drug carriers: Influence of various solvents on the formation of particles and sustained release of Indomethacin. *Biotechnology and Bioprocess Engineering*, *9*, 476–481.
Lee, C., Lim, S., Kim, G., Kim, D. W., Rhee, J. H., & Lee, K. (2005). Rosin nanoparticles as a drug delivery carrier for the controlled release of hydrocortisone. *Biotechnology Letters*, *27*, 1487–1490.
Lee, W., & Yeh, Y. (2005). Studies on preparation and properties of NIPAAm/hydrophobic monomer copolymeric hydrogels. *European Polymer Journal*, *41*, 2488–2495.
Liu, X., Xin, W., & Zhang, Z. (2009). Rosin based acid anhydrides to petrochemical curing agents. *Green Chemistry*, *11*, 1018–1025.
Kumar, P. T. S., Sirinivasan, S., Lakshmanan, V., Tamura, H., Nair, S. V., & Jayakumar, R. (2011). β-Chitin hydrogel/nano hydroxyapatite composite scaffolds for tissue engineering applications. *Carbohydrate Polymers*, *85*, 584–591.
Mastropeitro, D. J., Omidian, H., & Park, K. (2012). Drug delivery applications for superporous hydrogels. *Expert Opinion in Drug Delivery*, *9*, 71–89.
Mustata, F., & Bicu, I. (2010). A novel route for synthesizing esters and polyesters from the diels-alder adduct of levopimaric acid and acrylic acid. *European Polymer Journal*, *46*, 1316–1327.
Nande, V. S., Barabde, U. V., Morkhade, D. M., Patil, A. T., & Joshi, S. B. (2006). Synthesis and characterization of PEGylated derivatives of rosin for sustained drug delivery. *Reactive and Functional Polymers*, *66*, 1373–1383.
Pandey, M., & Amin, M. C. I. M. (2013). Accelerated preparation of novel bacterial cellulose/acrylamide-based hydrogel by microwave irradiation. *International Journal of Polymeric Materials and Polymeric Biomaterials*, *62*, 402–405.
Pekel, N., Yoshii, F., Kume, T., & Guven, O. (2004). Radiation crosslinking of biodegradable hydroxy propyl methyl cellulose. *Carbohydrate Polymers*, *55*, 139–147.
Shukla, R. K., & Tiwari, A. (2012). Carbohydrate polymers: Applications and recent advancements in delivering drugs to colon. *Carbohydrate Polymers*, *88*, 399–416.
Spoljaric, S., Salminen, A., Luong, N. D., & Seppälä, J. (2013). Crosslinked nanofibrillated cellulose: Poly(acrylic acid) nanocomposite films; enhanced mechanical performance in aqueous environments. *Cellulose*, *20*, 2991–3005.
Wang, H., Gurau, G., & Rogers, R. D. (2012). Ionic liquid processing of cellulose. *Chemical Society Reviews*, *41*, 1519–1537.
Wang, J., Yao, K., Wang, C., Tang, C., & Jiang, X. (2013). Synthesis and drug delivery of novel amphiphilic block copolymers containing hydrophobic dehydroabietic moeity. *Journal of Materials Chemistry B*, *1*, 2324–2332.
Xu, X., Duan, W., Huang, M., & Li, G. (2011). Synthesis of cellulose dehydroabietate in ionic liquid [bmim]Br. *Carbohydrate Research*, *346*, 2024–2027.
Yao, F., Zhang, D., Zhang, C., Yang, W., & Deng, J. (2013). Preparation and application of abietic acid-derived optically active helical polymers and their chiral hydrogel. *Bioresource Technology*, *123*, 58–64.
Yoshii, F., Zhao, L., Wach, R. A., Nagasawa, N., Mitomo, H., & Kume, T. (2003). Hydrogels of polysaccharide derivatives crosslinked with irradiation at paste-like condition. *Nuclear Instruments and Methods in Physics Research B*, *208*, 320–324.
Zhang, Z., Chen, L., Zhao, C., Bai, Y., Deng, M., Shan, M., et al. (2011). Thermo- and pH-responsive HPC-g-AA/AA hydrogels for controlled drug delivery applications. *Polymer*, *52*, 676–682.
Zhao, H., Kwak, J., Zhang, C., Brown, H. M., Arey, B. W., & Holladay, J. E. (2007). Studying cellulose fiber structure by SEM, XRD NMR and acid hydrolysis. *Carbohydrate Polymers*, *68*, 235–241.